EVS24
Stavanger, Norway, May 13-16, 2009

Design and Implementation of a Thermoelectric-Photovoltaic Hybrid Energy Source for Hybrid Electric Vehicles

Xiaodong Zhang, K. T. Chau, and C. C. Chan
Department of Electrical and Electronic Engineering, the University of Hong Kong, Hong Kong, China
xiaodong@eee.hku.hk

Abstract

In recent years, there is active research on exhaust gas waste heat energy recovery for hybrid electric vehicles (HEVs). Meanwhile, the use of solar energy in HEVs is also proposed to promote on-board renewable energy and hence improve their fuel economy. In this paper, a new thermoelectric-photovoltaic (TE-PV) hybrid energy source system is proposed and implemented for HEVs. The key is to newly develop the power conditioning circuit and its maximum power point tracking so that the output power of the proposed TE-PV hybrid energy source can be maximized. An experimental system is prototyped and tested to verify the validity of the proposed TE-PV hybrid energy source.

Keywords: HEV, on-board, DC-DC, converter, energy recovery.

1 Introduction

With ever-increasing oil consumption and concern of environmental protection, there is fast growing interest in hybrid electric vehicles (HEVs) globally [1]. Compared to the internal combustion engine vehicle (ICEV), the HEV is more energy efficient due to the optimization of engine operation mode and recovery of kinetic energy into electricity [2]. Moreover, more electrical energy from the vehicle system can satisfy the higher electricity demand because of the installation of the air condition, the safety control system, and other miscellaneous vehicle-borne electronic devices [3]. So there is a pressing need to develop energy-efficient power sources for HEVs, including the on-board renewable energy [4] and hybrid energy sources [5], with current renewable energy technologies, such as the waste heat recovery technology [6]-[8], wind energy [9]-[15], solar energy conversion [16], [17], and etc.

As shown in Fig. 1, in a typical energy flow path of the ICEV, only about 25% of the fuel combustion energy is utilized to propel the vehicles, whereas about 40% is wasted in the form of waste heat of exhaust gas [7], [18]. It means that the fuel economy of ICEV can be increased by up to 20% simply by capturing the waste heat of exhaust gas and converting about 10% of it to electricity with thermoelectric (TE) modules. Consequently, the research on waste heat energy recovery of the exhaust gas in HEVs has been actively conducted in recent years [3], [6], and [18]-[20]. Furthermore, the thermoelectric generator (TEG) has unique advantages of being maintenance free, silent in operation, independent on weather or topography and involving no moving and complex mechanical parts, compared with other power generators like gasoline generator, and wind turbine [21]-[24].

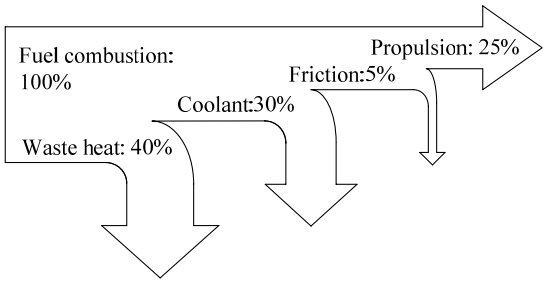

Figure 1: Typical energy flow path in an ICEV.

Benefited from the Seebeck effect, the TE modules can directly convert the heat energy to electrical energy. However, since the output power characteristics of the TEG are highly nonlinear and heavily depend on the heat source, cooling system, and external load, a proper power conditioning circuit and maximum power point tracking (MPPT) control are required [3]. On the other hand, the use of solar energy has been proposed for HEVs so as to promote the concept of on-board renewable energy and hence further improve their fuel economy. However, similar to those of the TEG, the output power characteristics of the photovoltaic (PV) panel are highly nonlinear and heavily depend on the irradiance, ambient temperature, and external load, a proper power conditioning circuit and MPPT control are also required.

Unfortunately, the PV panel and TEG need to be separately operated now, even though they are installed in a same HEV. It means that two set of controlling units, DC-DC converters, charging battery packs, and even DC-AC inverters are needed at more cost, weight, and volume. Compared with the single TE or PV energy source, the TE-PV hybrid energy source can offer some definite advantages, namely the higher fuel economy due to the increase of on-board renewable energy, the better energy security due to the use of multiple energy sources, and the higher control flexibility due to the coordination for charging the same pack of batteries. So the newly proposed TE-PV hybrid energy source is promising for the application to HEVs, as shown in Fig. 2.

A number of topologies of power conditioning circuits for small scale power generators have been proposed in the last decades [25]-[30]. For example, several dc-dc converter topologies have been proposed for TE conversion, such as the Ćuk converter [3], the SEPIC converter [8] and the boost-buck cascade converter [31], [32]. However, these topologies can not meet the requirements of the hybrid energy sources. The multiple-input converters (MICs) can be used to interface the energy sources and the load as the power conditioning circuit [33]. This class of DC-DC converters can simultaneously handle multiple inputs, and regulate the output voltage or current. Nevertheless, the MIC topology suitable for the TE-PV hybrid energy source is still absent in literature.

Considering the special requirements of energy source in HEVs, the topology of the TE-PV hybrid energy source must qualify the following features. Firstly, the input voltage from the TEG or PV panel may widely and dynamically vary according to specific external physical factors. So a large range of input voltage variation caused by different temperature difference and insolation is acceptable. Secondly, the hybrid energy system needs to charge the battery or directly supply electrical energy to the vehicle power network. Since the input voltage changes in a wide range, a dc-dc converter, having step-up and step-down characteristics, is required to serve for power conditioning. For example, the output voltage range of typical TEG is 0-25 V, which needs to be converted to 12.3-16.5 V for battery charging [32]. Thirdly, the MPPT can be realized for both TEG and PV panel. At last, the power from TEG and PV panel can be delivered to the load individually or simultaneously.

In order to fully utilize the TEG and PV panel, various MPPT algorithms have been applied, such as the load matching method [34], the curve-fitting scheme [35], the incremental conductance technique [36], the ripple correlation algorithm [37], and the perturbation and observation (PAO) method [38]. Moreover, the fuzzy logic [39] and

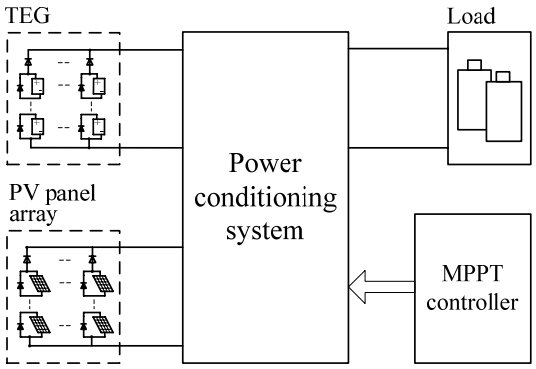

Figure 2: The proposed hybrid energy system.

neural network [40] have also been adopted for MPPT. The PAO method is one of the common used MPPT algorithms in practice because of its simplicity and system independence.

In this paper, a new TE-PV hybrid energy source system is proposed and implemented for HEVs. A MIC topology which consists of two single ended primary inductor converters (SEPICs) in parallel and a MPPT control strategy which enables both the TEG and the PV panel simultaneously achieving the maximum output power are proposed. The analysis shows that the power conditioning circuit can satisfy the requirements of the TE-PV hybrid energy system. Both theoretical derivation and experimental verification are given to support the validity of the proposed system.

2 Photovoltaic Panel and Thermoelectric Generator

Assuming that the contact loss and the output characteristics between the conversion elements of same type are ignorable, the model of the TEG and PV panel can be simplified as a single TE module model and a single PV panel model, proportionally with the corresponding numbers in series or in parallel.

The equivalent circuit of a PV panel is shown in Fig. 3. Normally, the PV panel is regarded as a current source shunted by a diode with a series resistor and a parallel resistor. Its numerical description is given by:

$$I = I_L - I_0\left\{\exp\left[\frac{q(V+IR_S)}{AKT}\right]-1\right\}-\frac{V+IR_S}{R_{Sh}}, \qquad (1)$$

where I and V are the output current and output voltage of the PV panel, respectively, I_L is the generated current under a given insolation, I_0 is the reverse saturation current, q is the charge of an electron, A is the ideality factor for a p-n junction, K is the Boltzmann constant, T is the absolute temperature, and R_S and R_{Sh} are the intrinsic series and parallel resistance, respectively.

As the irradiance decreases, the output power and the short circuit current of the solar panel will decline, while the internal resistance increases. When the surface temperature keeps rising, the open circuit voltage will decrease, and deteriorate the output power slightly. The interconnection of the PV panel array is shown in Fig. 4. In the PV panel array, each panel is paralleled with a by-pass diode to bypass the possibly failed solar panel. And at each panel strings, a diode is connected to avoid the electricity flowing back from the battery or circulating between the parallel strings.

The equivalent circuit of a TE module is simply represented by a voltage source connecting with an internal resistor in series. Both the internal resistance and the output power of the TE material increase with the temperature difference across the TE modules. Similarly, the interconnection of the TE modules is configured like that of the PV panel array.

Using the Thevenin's theorem, the TEG or PV panel array can be simply represented by a voltage source with an internal resistor. The power conditioning circuit can track the maximum power point (MPP) of the energy source by tuning its duty cycle of the switching PWM signal to ensure the input resistance $r_{in} = V_i / I_i$ equal the internal resistor of the energy source r_g, as shown in Fig. 5.

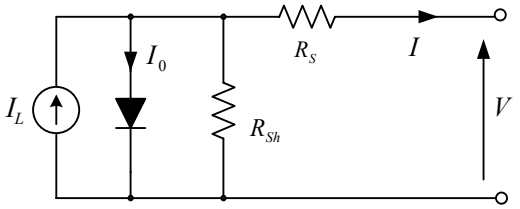

Figure 3: The equivalent circuit of a solar panel.

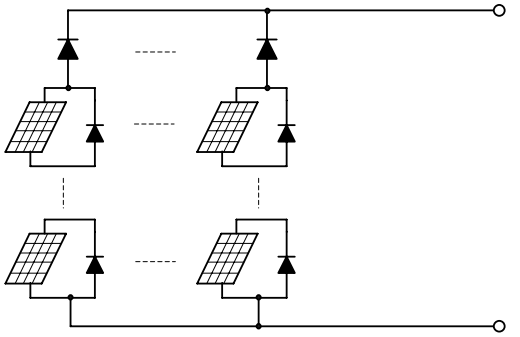

Figure 4: The interconnection of the PV panel array.

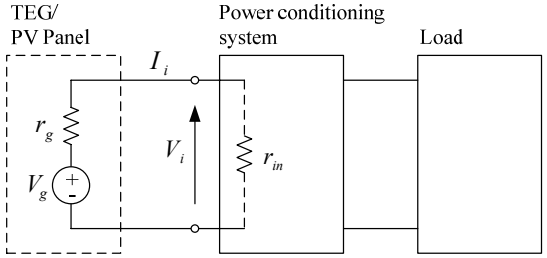

Figure 5: The power conditioning circuit.

3 TE-PV Hybrid Energy System

3.1 SEPIC in Discontinuous Capacitor Voltage Mode

According to the previously mentioned criteria of the hybrid energy system, the SEPIC circuit in Fig. 6 is preferable to serve as the power conditioning circuit. The SEPIC have step-up and step-down characteristics with wide input voltage. Furthermore, the SEPIC has low-ripple input current and inherent input-output galvanic isolation.

The SEPIC is mainly operated in three modes: continuous current mode (CCM), discontinuous inductor current mode (DICM), and discontinuous capacitor voltage mode (DCVM) [41]. Generally speaking, the CCM is relatively more suitable for converting high voltage, high current input application, the DICM is for high voltage, low current input application, and the DCVM is for low voltage, high current input application [42]. Since TEG or PV panel are low voltage inputs and the charging battery is high current energy storage unit, the SEPIC circuit is kept in DCVM mode in the following analysis.

Supposing the inductor inductors L_1, L_2, and the output capacitor C_{out} are big enough to guarantee that the currents I_1, I_2, and output voltage V_o are stable, the operating stages and key waveforms of SEPIC in DCVM are depicted in Fig. 7 and 8. During time interval $0 < t < dT_s$ in Fig. 7 (a), the input power source, the intermediate capacitor, and the output capacitor charge the inductors L_1, L_2, and the load R, respectively. When the voltage of C_s decreases below than $-V_o$, the diode D starts to conduct at time $t = dT_s$. Then, the inductor L_2 charges the output capacitor and load whilst the input power source charges the inductor L_1 until time $t = DT_s$ in Fig. 7 (b). When the switch S is turned off $DT_S < t < T_s$ in Fig. 7 (c), the inductors L_1 and L_2 charge the load together. Based on the previous analysis, the voltage function of the intermediate capacitor $v_{cs}(t)$ can be expressed as:

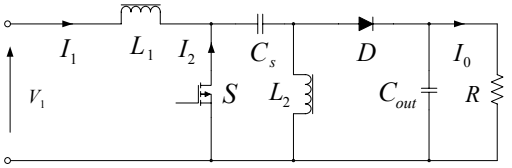

Figure 6: Circuit diagram of the SEPIC circuit.

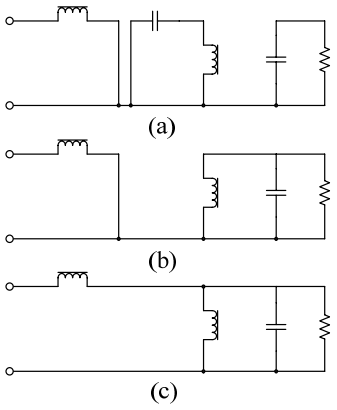

Figure 7: Operating stages of the SEPIC circuit.

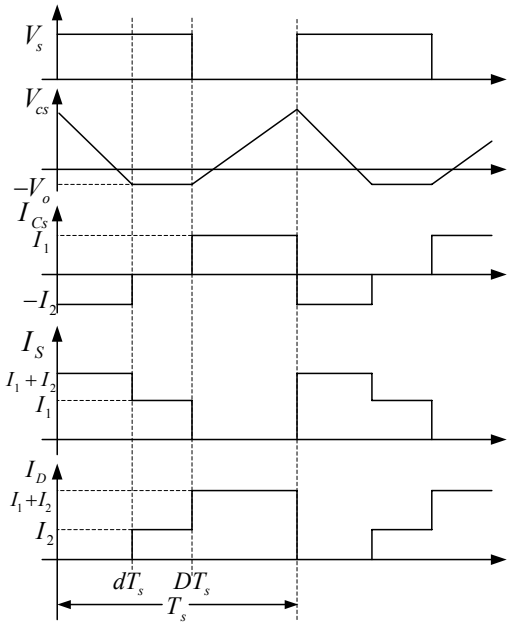

Figure 8: Key waveforms of the SEPIC circuit.

$$v_{cs}(t)=\begin{cases}\dfrac{I_1(1-D)T_s}{C_s}-V_o-\dfrac{I_2 t}{C_s}, & 0<t<dT_s\\ -V_o, & dT_s<t<DT_s\\ -V_o+\dfrac{I_1(t-DT_s)}{C_s}, & DT_s<t<T_s.\end{cases} \quad (2)$$

At the steady state of the circuit, the average voltages of L_1 and L_2 and the average current of C_s equal zero. It implies that the average currents I_1, I_2, and the average voltage of C_s are equal to input current I_i, output current I_o, and input voltage V_i, respectively. So the input voltage is

$$V_i=\frac{1}{T_s}\int_0^{T_s} v_c(t)dt=\frac{T_s}{2C_s}I_1(1-D)^2. \quad (3)$$

Then, the input resistance of the SEPIC in DCVM is

$$r_{in}=\frac{T_s(1-D)^2}{2C_s}. \quad (4)$$

By adjusting the duty cycle of the switching PWM signal of S, the input resistor of the SEPIC can match the internal resistor of the TEG or PV panel array to extract the maximum power.

As shown in Fig. 8, the ampere-second balance on C_s is expressed as:

$$I_1(1-D)T_s=I_2 dT_s. \quad (5)$$

Since the input power and output power balance each other, that is, $V_iI_1=V_oI_2$, the voltage conversion ratio M is described as:

$$M=\frac{V_o}{V_i}=\frac{I_1}{I_2}=\frac{d}{1-D}. \quad (6)$$

And the input power balances the power dissipated on the load, that is, $V_iI_1=V_o^2/R$. From (6), it gets

$$d=\sqrt{2RC_sf_s}, \quad (7)$$

where f_s is the switching frequency, $f_s=1/T_s$. Obviously, the DCVM mode can be ensured if $D>d$. From (6) and (7), the criterion of the load to ensure the DCVM for SEPIC is given by:

$$2RC_sf_s\le\left(\frac{M}{M+1}\right)^2. \quad (8)$$

By setting the inequality formula (8) to an equality formula $2RC_sf_s=\left(\frac{M}{M+1}\right)^2$, the critical load R^* can be computed easily. Because the functions at both sides are monotonous increasing functions with respect to the variable R, the load criterion will just be $R\le R^*$.

3.2 System Configuration

Based on the facts and equations of the SEPIC in DCVM, the hybrid TE-PV energy system is studied to extract maximum power of the whole system. The circuit diagram of the hybrid energy system is shown in Fig. 9. The syntheses of the SEPIC-SEPIC MIC are done by connecting the pulsating current source of the SEPIC converter into another SEPIC in parallel.

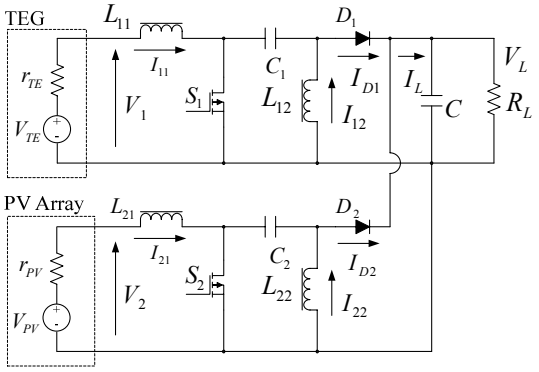

Figure 9: Circuit diagram of hybrid energy system.

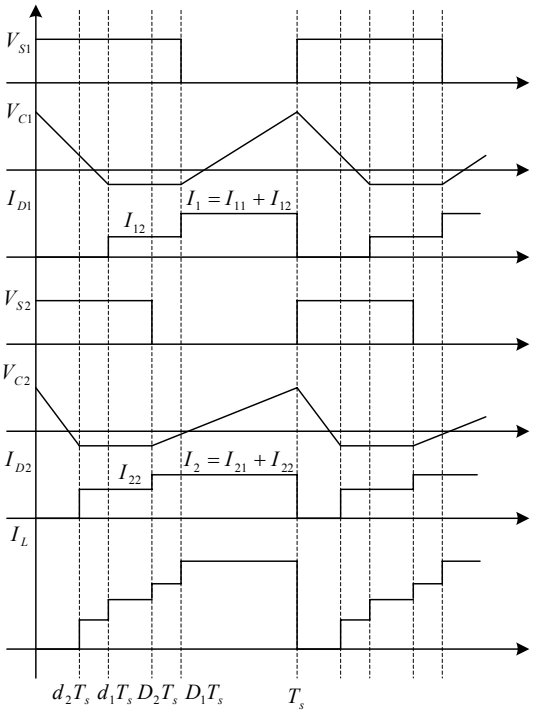

Figure 10: Key waveforms of hybrid energy system.

With the big enough inductors and output capacitor, from (3) and (4), it is obvious that the input resistor of each branches does not directly associated with the load R_L. It means that the MPP can be tracked exactly the same as the single SEPIC circuit if and only if the two branches are both in DCVM. Set the parameters of the duty cycles of each branches as d_1T_s and D_1T_s for TEG branch, and as d_2T_s and D_2T_s for PV panel branch. The key waveforms of the hybrid energy system are explicated in Fig. 10. Since the input resistances of two branches can be adjusted separately, the PAO method is used separately to track the MPPs of the TEG branch and PV panel branch.

4 Experimental Results

At the beginning of the experiment, the output characteristics of the TEG and PV panel are measured at specific working conditions by changing a rheostat as the external load. The TEG branch of the hybrid system includes 18 pieces of Bi-Te TE modules (Model TEP1-12656-0.6), a 3.5 kW induction heater, and a water cooling system. These TE modules are connected as 6 pieces electrically in series and 3 branches in parallel. When the temperature of the cold-side is fixed at around 50℃, the output characteristics of the TEG are recorded at different hot-side temperatures, 120℃, 170℃, and 220℃, as shown in Fig. 11.

The PV panel branch has 9 pieces of polycrystalline-silicon PV panels (Model SR10-36), 20 pieces of tungsten halogen lamps, and an AC transformer to adjust the irradiance. Nine pieces of PV panels are connected electrically in parallel. With the surface temperature of around 40 ℃, the output characteristics of the PV panel are shown in Fig. 12.

It is obvious that the output power of TEG and PV panel are heavily dependent on the external physical factors. The power output of the TEG and PV panel increase as the increasing of the irradiance and temperature difference, respectively. With varying external load, the output power changes significantly. These figures show the necessity of the power conditioning circuit. At the same time, the internal resistances of TEG and PV panel can be obtained, which equal the resistance of the rheostat at the MPPs.

With the measured output characteristics of the TEG and PV panel, the SEPICs of each branch can be designed according to the equations in previous section. By tuning the duty cycle of the SEPIC switching single, the MPP can be tracked at each branch, as shown in Fig. 13.

The hybrid energy system with MPPT control is implemented including the TEG, PV panel, SEPIC-SEPIC converter, DSP controller, and a 12V, 24Ah charging battery as the load. In the experiment, the initial duty cycle of the switching signal is 40%, and the Δd is set as 0.5%. The starting of the hybrid energy system is illustrated in Fig. 14. In order to test the dynamic performance of the hybrid system, a 10 ohm resistor load is paralleled connected with a 12 ohm resistor at 10 s. From Fig. 15, it can see that the PV output power is very stable in the whole process.

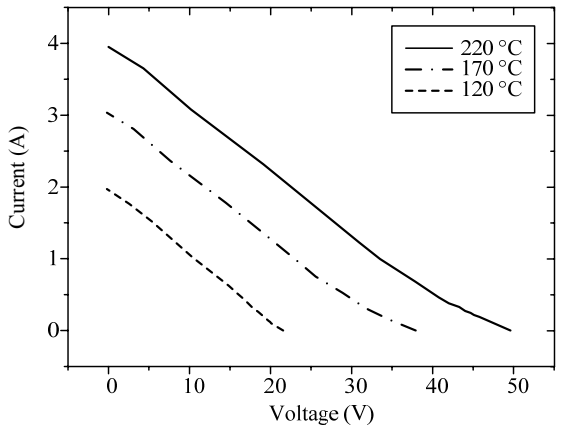

(a) Current versus voltage.

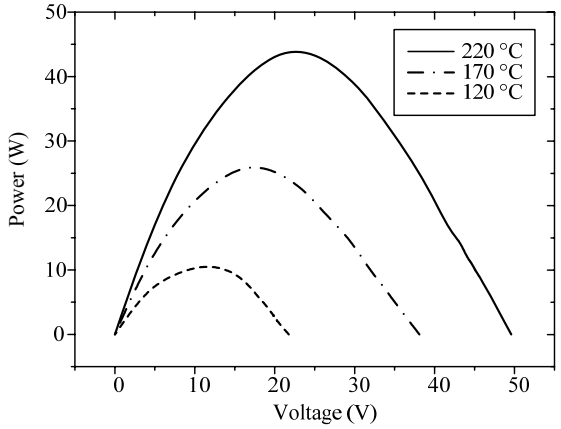

(b) Output power versus voltage.

Figure 11: Output characteristics of TEG branch.

As shown in Fig. 15, the dynamic response of the PV system is very quick to react with the irradiance change. Since the time constant of the TEG system is much larger than that of the PV panel system, so the response of the proposed hybrid system can satisfy the requirement for both branches.

In order to verify the MPPT control method, the comparison is carried out. One is giving a fixed PWM driving signal with 50kHz frequency and 65% duty cycle to the system; the other one is drived by the MPPT controller with a PWM signal at constant 45 kHz and initial duty cycle 65%. The reason to choose 65% is that MPP of both branches can be closely achieved at the same time according to Fig.13. The result in Fig. 16 shows that the TE-PV hybrid energy system can achieve MPP, hence the maximum power will be transferred to the battery under all different changing external factors.

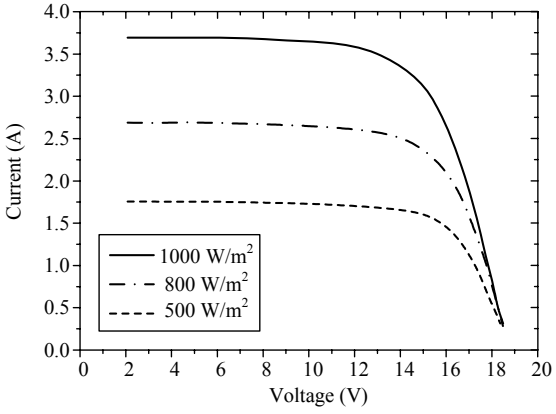

(a) Current versus voltage.

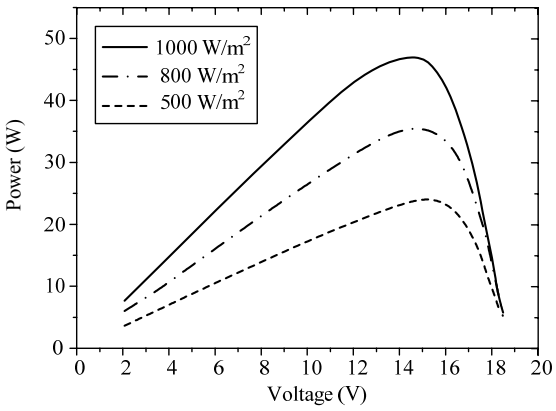

(b) Output power versus voltage.

Figure 12: Output characteristics of PV panel branch.

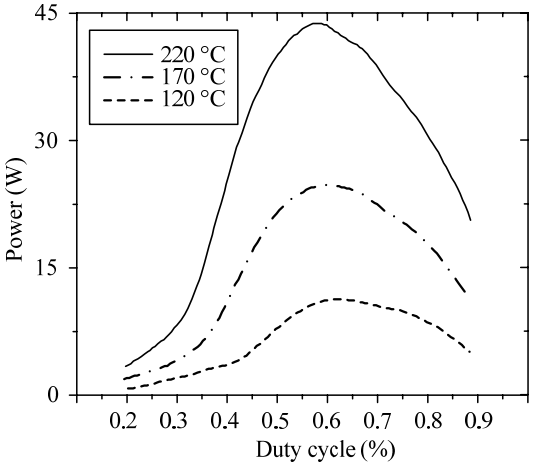

(a) TEG output power.

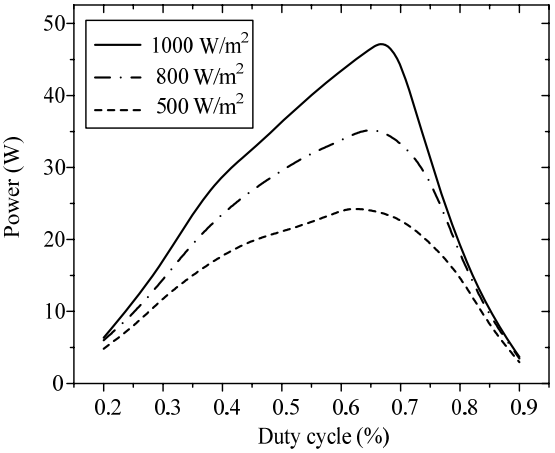

(b) PV panel array output power.

Figure 13: The output power versus the duty cycle of SEPIC branches.

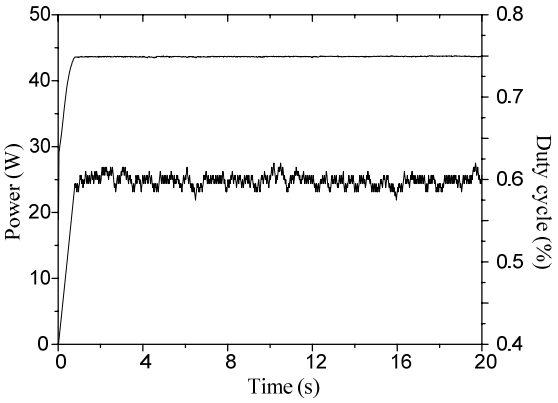

(a) TEG output power with MPPT.

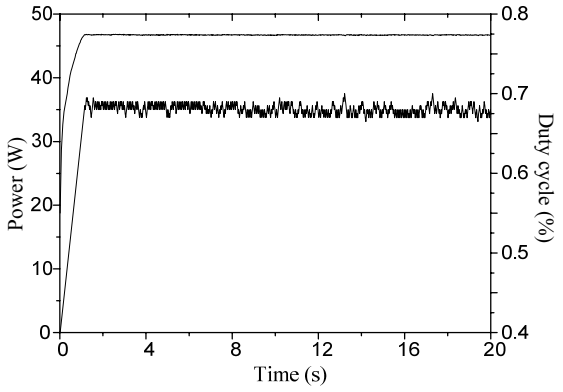

(b) PV panel output power with MPPT.

Figure 14: Output power with MPPT (Upper line is output power value, and lower line is duty cycle).

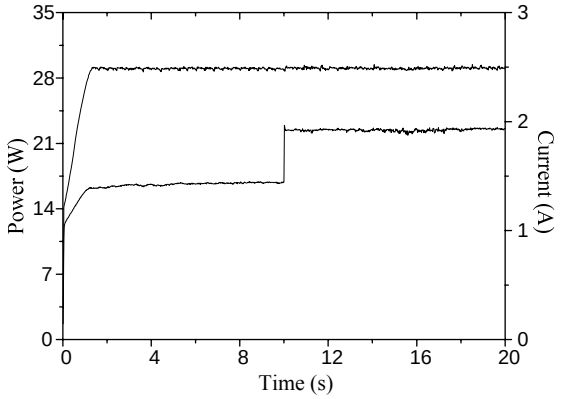

Figure 15: Output power at changed load (Upper line is output power value, and lower line is output current).

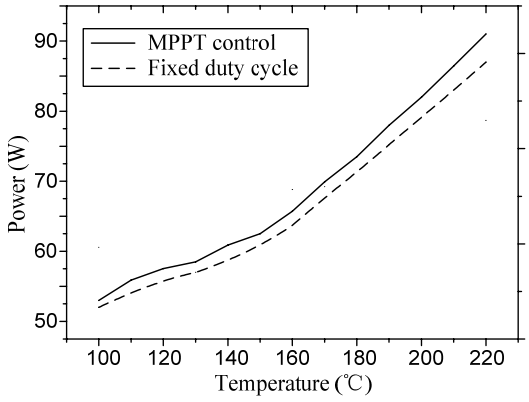

Figure 16: Comparison of output power.

5 Conclusion

Compared with the individual energy system, the hybrid power system can provide more merits. But the topology of the hybrid TE-PV has special requirements. The SEPIC-SEPIC MIC circuit can satisfy the requirement of the hybrid energy system. In this paper, the hybrid TE-PV energy system is proposed and verified at an around 100W test bed. The hybrid energy system can achieve the whole MPP simultaneously or the individual MPP separately. The operating modes, the MPPT implement are investigated.

Acknowledgments

This work was supported in part by a grant (HKU 7105/07E) from the Research Grants Council and a grant (Project code: 200807176032) from the Committee on Research and Conference Grants, The University of Hong Kong, Hong Kong Special Administrative Region, China.

References

[1] K. T. Chau and C. C. Chan, *Emerging energy-efficient technologies for hybrid electric vehicles*, Proceedings of the IEEE, Vol. 95, No. 4, Apr. 2007, pp. 821-835.

[2] C. C. Chan, *The state of the art of the electric, hybrid, and fuel cell vehicles*, Proceedings of the IEEE, Vol. 95, No. 4, Apr. 2007, pp. 704-718.

[3] C. Yu, K. T. Chau and C. C. Chan, *Thermoelectric waste heat energy recovery for hybrid electric vehicles*, Proceedings of 23rd International Electric Vehicle Symposium, Dec. 2007, Paper No. 21.

[4] K. T. Chau, Y. S. Wong and C. C. Chan, *An overview of energy sources for electric vehicles*, Energy Conversion and Management, Vol. 40, No. 10, July 1999, pp. 1021-1039.

[5] K. T. Chau and Y. S. Wong, *Hybridization of energy sources in electric vehicles*, Energy Conversion and Management, Vol. 42, No. 9, June 2001, pp. 1059-1069.

[6] X. Zhang, K. T. Chau and C. C. Chan, *Overview of thermoelectric generation for hybrid vehicles*, Journal of Asian Electric Vehicles, Vol. 6, No. 2, Dec. 2008, pp. 1119-1124.

[7] D. M. Rowe, *Thermoelectrics, an environmentally-friendly source of electrical power*, Renewable Energy, Vol. 16, No. 1-4, Jan./Apr. 1999, pp. 1251-1256.

[8] J. Eakburanawat and I. Boonyaroonate, *Development of a thermoelectric battery-charger with microcontroller-based maximum power point tracking technique*, Applied Energy, Vol. 83, No. 7, July 2006, pp. 687-704.

[9] Y. Fan, K. T. Chau and M. Cheng, *A new three-phase doubly salient permanent magnet machine for wind power generation*, IEEE Transactions on Industry Applications, Vol. 42, No. 1, Jan./Feb. 2006, pp. 53-60.

[10] Y. Fan, K. T. Chau and S. Niu, *Development of a new brushless doubly fed doubly salient machine for wind power generation*, IEEE Transactions on Magnetics, Vol. 42, No. 10, Oct. 2006, pp. 3455-3457.

[11] K. T. Chau, Y. B. Li, J. Z. Jiang and S. Niu, *Design and control of a PM brushless hybrid generator for wind power application*, IEEE Transactions on Magnetics, Vol. 42, No. 10, Oct. 2006, pp. 3497-3499.

[12] S. Niu, K. T. Chau, J. Z. Jiang and C. Liu, *Design and control of a new double-stator cup-rotor permanent-magnet machine for wind power generation*, IEEE Transactions on Magnetics, Vol. 43, No. 6, June 2007, pp. 2501-2503.

[13] C. Yu, K. T. Chau and J. Z. Jiang, *A flux-mnemonic permanent magnet brushless machine for wind power generation*, Journal of Applied Physics, Vol. 105, No. 7, Apr. 2009, Paper No. 07F114, pp. 1-3.

[14] L. Jian, K. T. Chau and J. Z. Jiang, *A magnetic-geared outer-rotor permanent-magnet brushless machine for wind power generation*, IEEE Transactions on Industry Applications, Vol. 45, No. 3, May/June 2009.

[15] K. T. Chau, C. C. Chan and C. Liu, *Overview of permanent-magnet brushless drives for electric and hybrid electric vehicles*, IEEE Transactions on Industrial Electronics, Vol. 55, No. 6, June 2008, pp. 2246-2257.

[16] J. Schaefer, *Review of photovoltaic power plant performance and economics*, IEEE Transactions on Energy Conversion, Vol. EC-5, June 1990, pp. 232-238.

[17] H. S. H. Chung, K. K. Tse, S. Y. R. Hui, C. M. Mok and M. T. Ho, *A novel maximum power point tracking technique for solar panels using a SEPIC or Ćuk converter*, IEEE Transactions on Power Electronics, Vol. 18, No. 3, May 2003, pp. 717-724.

[18] F. Stabler, *Automotive applications of high efficiency thermoelectrics*, Proceedings of DARPA/ONR Program Review and DOE High Efficiency Thermoelectric Workshop, Mar. 2002, pp. 1-26.

[19] J. Yang, *Potential applications of thermoelectric waste heat recovery in the automotive industry*, International Conference on Thermoelectrics, Jun. 2005, pp. 155-159.

[20] X. Zhang, K. T. Chau, C. Yu and C. C. Chan *An optimal solar-thermoelectric hybrid energy system for hybrid electric vehicles*, IEEE Vehicle Power and Propulsion Conference, Sep. 2008, pp. 1-6.

[21] C. Liu, K. T. Chau, J. Z. Jiang and L. Jian, *Design of a new outer-rotor permanent magnet hybrid machine for wind power generation*, IEEE Transactions on Magnetics, Vol. 44, No. 6, June 2008, pp. 1494-1497.

[22] S. Niu, K. T. Chau and J. Z. Jiang, *Analysis of eddy-current loss in a double-stator cup-rotor PM machine*, IEEE Transactions on Magnetics, Vol. 44, No. 11, Nov. 2008, pp. 4401-4404.

[23] C. Liu, K.T. Chau, J.Z. Jiang and S. Niu, *Comparison of stator-permanent-magnet brushless machines*, IEEE Transactions on Magnetics, Vol. 44, No. 11, Nov. 2008, pp. 4405-4408.

[24] S. Niu, K.T. Chau and C. Yu, *Quantitative comparison of double-stator and traditional permanent magnet brushless machines*, Journal of Applied Physics, Vol. 105, No. 7, Apr. 2009, Paper No. 07F105, pp. 1-3.

[25] Y. Xue, L. Chang, S. B. Kjar, J. Bordonau, and T. Shimizu, *Topologies of single-phase inverters for small distributed power generators: an overview*, IEEE Transactions on Power Electronics, Vol. 19, No. 5, Sep. 2004, pp. 1305-1314.

[26] K. T. Chau, *New constant-frequency multi-resonant boost convertor*, IEE Electronics Letters, Vol. 30, No. 2, Jan. 1994, pp. 101-102.

[27] M. S. W. Chan, K. T. Chau and C. C. Chan, *A new switched-capacitor inverter for electric vehicles*, Journal of Asian Electric Vehicles, Vol. 4, No. 2, Dec. 2006, pp. 905-909.

[28] K. T. Chau, *A new class of pulsewidth-modulated multi-resonant converters using resonant inductor freewheeling*, International Journal of Electronics, Vol. 77, No. 5, Nov. 1994, pp. 703-714.

[29] M. S. W. Chan and K. T. Chau, *A switched-capacitor boost-multilevel inverter using*

partial charging, IEEE Transactions on Circuits and Systems II, Vol. 54, No. 12, Dec. 2007, pp. 1145-1149.

[30] K. T. Chau, J. M. Yao and C. C. Chan, *A new soft-switching vector control approach for resonant snubber inverters*, International Journal of Electronics, Vol. 86, No. 1, Jan. 1999, pp. 101-115.

[31] R. Y. Kim, and J. S. Lai, *A Seamless Mode Transfer Maximum Power Point Tracking Controller for Thermoelectric Generator Applications*, Conference Record of the IEEE Industry Applications Conference, 42nd IAS Annual Meeting, Sep. 2007, pp. 977-984.

[32] R. Y. Kim, and J. S. Lai, *Aggregated modeling and control of a boost-buck cascade converter for maximum power point tracking of a thermoelectric generator*, The 23rd Annual IEEE Applied Power Electronics Conference and Exposition, Feb. 2008, pp. 1754-1760.

[33] Y. C. Liu and Y. M. Chen, *A systematic approach to synthesizing multi-input DC/DC converters*, IEEE Power Electronics Specialists Conference, June 2007, pp. 2626-2632.

[34] K. Khouzam, *Optimum load matching in direct-coupled photovoltaic power systems - application to resistive loads*, IEEE Transactions on Energy Conversion, Vol. 5, No. 2, 1990, pp. 265-271.

[35] A. Kislovski, and R. Redl, *Maximum-power-tracking using positive feedback*, Proceedings of IEEE Power Electronics Specialists Conference, June 1994, pp. 1065-1068.

[36] Y. C. Kuo, T. J. Liang, and J. F. Chen, *Novel maximum-power- point tracking controller for photovoltaic energy conversion system*, IEEE Transactions on Industrial Electronics, Vol. 48, No. 3, June 2001, pp. 594-601.

[37] D. Shmilovitz, *On the control of photovoltaic maximum power point tracker via output parameters*, IEE Proceedings on Electric Power Applications, Vol. 152, No. 2, Mar. 2005, pp. 239-248.

[38] N. Femia, G. Petrone, G. Spagnuolo, and M. Vitelli, *Optimization of perturb and observe maximum power point tracking method*, IEEE Transactions on Power Electronics, Vol. 20, No. 4, July 2005, pp. 963-973.

[39] M. Veerachary, T. Senjyu, and K. Uezato, *Neural-network-based maximum-power-point tracking of coupled-inductor interleaved- boost converter-supplied PV system using fuzzy controller*, IEEE Transactions on Industrial Electronics, Vol. 50, No. 4, Aug. 2003, pp. 749-758.

[40] N. S. D'Souza, L. A. C. Lopes, and X. Liu, *An intelligent maximum power point tracker using peak current control*, Proceedings of IEEE Power Electronics Specialists Conference, June 2005, pp. 172-177.

[41] D. Maksimovic and S. Cuk, *A unified analysis of PWM converters in discontinuous modes*, IEEE Transactions on Power Electronics, Vol. 6, No. 3, July 1991, pp. 476-490.

[42] K. K. Tse, M. T. Ho, Henry S. H. Chung, and Ron S. Y. Hui, *A novel maximum power point tracker for PV panels using switching frequency modulation*, IEEE Transaction on Power Electronics, Vol. 17, No. 6, Nov. 2002, pp. 980-989.

Authors

Mr. Xiaodong Zhang received his B.Eng. and M.Eng. degrees from Department of Automation, Tianjin University, China, in 2002 and 2005 respectively. He is currently pursuing his Ph.D. degree in the University of Hong Kong. His research interests include the application of renewable energy sources and power electronics.

Prof. K. T. Chau is the professor in Department of Electrical and Electronic Engineering and Director of International Research Centre for Electric Vehicles at the University of Hong Kong. His research interests are electric vehicles, machines & drives, clean energy and power electronics. In these areas, he has published over 300 refereed technical papers. Prof. Chau is also a Fellow of IET.

Prof. C. C. Chan is currently an honorary professor in the University of Hong Kong. He has authored 4 books, published over 120 technical papers, and held 7 patents. Prof. Chan is also a Fellow of the Royal Academy of Engineering, U.K., an Academician of the Chinese Academy of Engineering, the Ukraine Academy of Engineering Science, and both IEEE and IET.